# Condensed phase effects on the electronic momentum distribution in the warm dense matter regime

Brian A. Mattern, Gerald T. Seidler,* and Joshua J. Kas
*Department of Physics, University of Washington, Seattle, WA 98195-1560*
(Dated: February 26, 2022)

We report *ab initio* calculations of the valence electron momentum distribution function $n(p)$ and dynamic structure factor for warm dense Be at Mbar pressures. We observe an unexpected, strong reshaping of the Compton profile upon increasing density, even well before any significant core-wavefunction overlap or electride behavior occurs. We propose that this nonperturbative effect, which is due to a growing influence on $n(p)$ of the orthogonalization of valence and core electron wavefunctions with increasing density, is observable by inelastic x-ray scattering at x-ray free-electron lasers and large-scale laser-shock heating facilities, and may also be more generally important for thermodynamic properties of dense, partially-ionized plasmas.
(submitted Phys. Rev. Lett. Aug. 2013)

arXiv:1308.2990v2 [physics.plasm-ph] 15 Aug 2013

There is growing interest in dense states of matter intermediate between traditional condensed phase systems and fully-ionized dense plasmas. These "warm dense matter" (WDM) states present unique scientific opportunities with special relevance to planetary and stellar conditions[1–4], with obvious importance for the early stages of compression in inertial confinement fusion (ICF)[5], and with additional broad, long-term scientific potential when considered as the next-stage of evolution of the available thermodynamic parameter space for the condensed phase community.

As with any new material regime, one must determine the dominant microphysics that establishes the resulting (macroscopic) thermodynamic and statistical properties. For WDM, this is complicated by the lack of simplifying features present in either the cold, ordered limit of condensed matter or the hot, non-degenerate limit of fully-ionized dilute plasmas; unsurprisingly, at present, no broadly-applicable, first-principles treatment of WDM is available. One must instead combine methods from these opposing limits[6–10] and then seek comparison with the limited, but growing, body of WDM experimental results.

As a case in point, a common theoretical approach to WDM[6, 11, 12] treats free or ionized electrons in the random phase approximation (RPA)[13] with perturbative corrections for the electron-ion scattering via the Born-Mermin approximation (BMA)[14, 15]. This approach necessarily assumes a weak electron-ion interaction and has seen extensive use in the interpretation of inelastic x-ray scattering from WDM[16–19].

By contrast, in crystalline materials and other condensed-phase systems it is the electron-ion interaction, both through the Coulombic potential and orthogonalization between core and valence electrons, that plays the dominant role in the overall electronic structure[20–22]. In addition, at elevated densities, where core wavefunctions begin to overlap, an interesting combination of free-energy effects constrained by valence-core orthogonalization (VCO) can lead to structural changes and novel phases known as electrides in which the valence electrons re-localize in the interstitial spaces between atomic sites[23–25]. This behavior at low temperatures hints at the possibility of strong influence of the electron-ion interaction, and in particular VCO, on the electronic structure of WDM. This conclusion, which runs contrary to the commonly stated perspective that the electron-ion interaction becomes progressively less important at high plasma densities[26], is further supported by the growing use in WDM molecular dynamics simulations of modern density-functional theory methods, such as projector-augmented wave calculations, that substantially include VCO effects[27, 28].

Here, we report a detailed theoretical study of the valence electron momentum distribution $n(p)$ for warm dense Be. In addition to being a candidate ablator material for ICF, and thus undergoing extensive study in the WDM context[16–18], Be has seen thorough high-resolution synchrotron study[29–32]. Our results illustrate that VCO, which has a long history in the context of electronic structure calculations[33, 34] and which plays an important role in determining the ambient momentum distribution of Be and other materials[35–38], steadily grows in importance upon increasing density. This observation may have significant consequences for calculation of the equation of state or thermodynamic susceptibilities (e.g., compressibility) for WDM but here we focus on an issue of central experimental importance: $n(p)$ is a primary experimental observable, appearing as a direct contributor to the dynamic structure factor measured by non-resonant inelastic x-ray scattering (NIXS) in the noncollective scattering regime and subsequently used to infer temperature and density of WDM[6].

NIXS experiments measure the dynamic structure factor $S(q,\omega)$ which determines the relative probability of transferring momentum $\hbar q$ and energy $\hbar\omega$ from the probe radiation to the sample in the scattering process[39]. At large $q$, the interpretation of NIXS simplifies due to the impulse approximation (IA)[40] wherein the potential be-

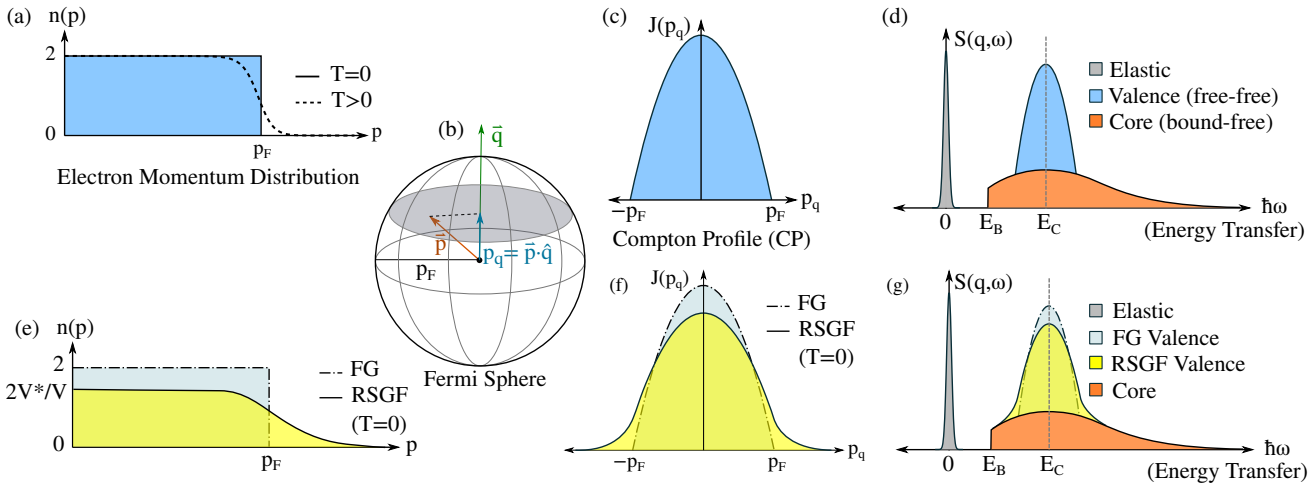



FIG. 1. Relationship between electronic momentum distribution and nonresonant IXS spectrum in the impulse approximation. (a)-(d): a non-interacting electron gas. (e)-(g) an electron gas with strong electron-ion interaction, such as due to valence-core orthogonalization (VCO). See the text for discussion.

fore and after the scattering process cancel implying that

$$\hbar\omega = \frac{\hbar^2 q^2}{2m} + \frac{\hbar\vec{q}\cdot\vec{p}}{m}, \tag{1}$$

where $\vec{p}$ is the scattering electron's initial momentum. This Doppler broadened Compton scattering is entirely determined by the electronic momentum distribution $n(p)$.

In Fig. 1 (a-d), we illustrate the relationship between $n(p)$ and the NIXS spectrum using a simple Fermi gas model for the valence electrons. In panel (a), we show the Fermi radial momentum distribution. This corresponds to the Fermi sphere shown in panel (b). In the shaded intersection between the Fermi sphere and a plane perpendicular to $\vec{q}$, the Doppler shift, and thus energy transfer, is identical. The area of this intersection as a function of displacement from the origin $p_q \equiv \vec{p}\cdot\hat{q}$ defines the Compton profile (CP) $J(p_q)$, shown in panel (c). According to Eq. (1), the CP is displaced by the Compton shift $E_C = \hbar^2 q^2/2m_e$ and stretched by $\hbar q/m$ to obtain $S(q,\omega)$. In panel (d), we show this along with a representative contribution from tightly-bound core electrons ($E_B$ is the core-state binding energy)[41].

Each of temperature, free-electron density, electron-electron interactions and electron-ion interactions influences $n(p)$. As shown in Fig. 1(e), interactions, if strong, have a global impact on $n(p)$ and the shape of the CP by moving occupation from states below the single-electron Fermi level to states above, even at $T = 0$. For an interacting Fermi gas at the density of ambient Be, electron-electron correlations result in a promotion of 5% of electrons to states above the Fermi level[42, 43]. As density increases, this effect diminishes. On the other hand, we show here that electron-ion interactions, which already have a stronger influence on electron occupation at ambient conditions[30, 37] (with 20% of electrons promoted above $p_F$[42]) have a growing, dramatic impact on $n(p)$ as density increases. This effect, and its consequences are shown schematically in Fig. 1 (e)-(g) and are presented in detail in the remainder of this letter.

In Fig. 2, we present calculations of the spherically-averaged radial momentum distribution $n(p)$ for hcp beryllium at $T = 0$ as a function of atomic density using a real-space Green's function (RSGF) method[45–47] that treats the electron-ion interaction non-perturbatively, including the effects of VCO. This is compared to calculations for a non-interacting Fermi gas (FG) and to calculations that include electron-ion interactions perturbatively via the BMA[14]. The distribution function shown in Fig. 2 is the number of electrons per momentum eigenstate $n(p)$, which is related to the momentum density $\rho(p)$ by $n(p) = ((2\pi)^3/V)\rho(p)$. The abscissa in Fig. 2 has been rescaled by the Fermi momentum, $p_F$ to capture the complete density-dependence of the Fermi gas n(p). The perturbative electron-ion interaction in the BMA results in a slight decrease in occupation at all momenta compensated for by increased occupation above $p_F$. Evidently, the bulk of the BMA density dependence is also captured by the rescaling by $p_F$. The RSGF calculations, on the other hand, show a marked density dependence differing from that of the free or weakly interacting FG. We note two primary features. First, $n(p)$ is nearly uniformly decreased at low $p$ and this depletion gets stronger with increased density. Second, the relative weight of the tail above $p_F$ increases with density.

In Fig. 3, we show Compton profiles that correspond to the momentum distributions from Fig. 2. The slight reshaping of the RSGF CP relative to the FG at am-

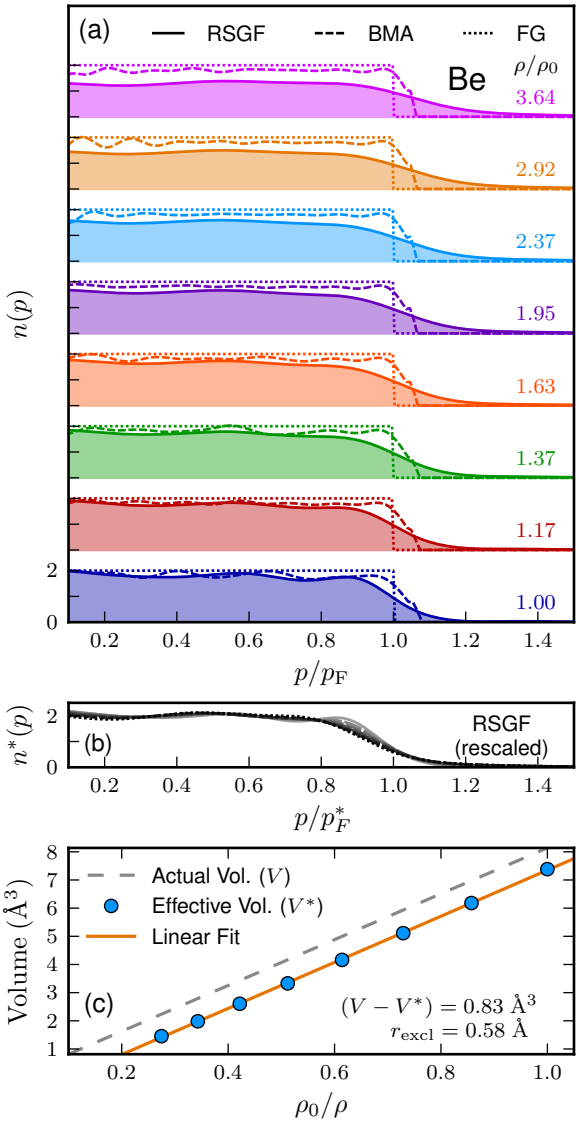



FIG. 2. Theoretical electronic momentum density of hcp Be as a function of atomic density $\rho$ in terms of ambient density $\rho_0$. The highest density shown corresponds to a pressure of $\sim$ 8 Mbar[44]. (a) Comparison between calculations using the non-perturbative real-space Green's function method (RSGF), the perturbative Born-Mermin approximation (BMA) and the non-interacting Fermi gas (FG). The momentum $p$ is scaled by the Fermi momentum $p_{\rm F}$. (b) RSGF calculations rescaled by an effective volume determined by the average occupation at low momenta. Curves at higher density are drawn darker. (c) The effective volume per atom as a function of inverse compression.

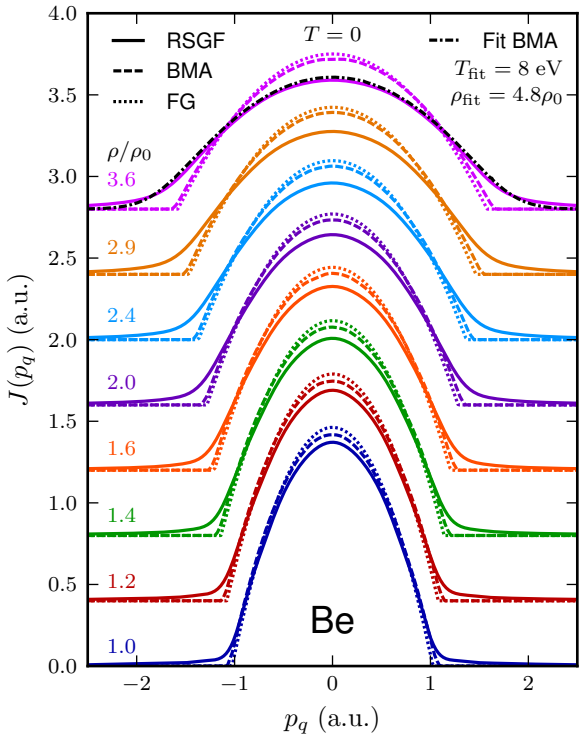



FIG. 3. Theoretical Compton profiles for Be metal as a function of density at T=0. The real-space Green's function (RSGF, solid curves) is compared to the Born-Mermin Approximation (BMA, dashed lines) and the Fermi gas (FG, dotted lines). In addition, for the highest density, we show the result of fitting a BMA calculation with adjustable temperature and density to the RSGF curve.

bient density is in good agreement with high-resolution experimental data[45]. As density increases, the differences between RSGF and FG become quite dramatic: the electron-ion interaction results in a significant reshaping of the CP, shifting weight from the peak out into the high-momentum tails.

The broad, nearly uniform depletion of valence occupation for $p < p_F$ indicates gross changes in the available phase space. Interestingly, these effects have a simple relationship to atomic density that suggests an overwhelming importance of VCO for $n(p)$ of solids or partially-ionized plasmas at high densities. In Fig. 2b we show a simple rescaling of all RSGF $n(p)$ by the apparent effective free volume per atom inferred from $\bar{n}$, the average occupancy of $n(p)$ at low $p$ (see Fig. 2c), i.e., $V^* = \bar{n}V/2$. The simple offset in the effective volume $V^*$ indicates that the overall phenomenon can be discussed, at least qualitatively, as an excluded volume effect encompassing the strong constraint imposed by VCO on the valence electron wavefunctions in the vicinity of the ion core. Numerically, $V_{\rm excl} = 0.83$ Å$^3$, which is the volume in which 98% of the $1s$ electrons are contained. There are clear similarities between these results, where VCO with Hartree-Fock bound states has been imposed, and the simpler hard-sphere model introduced by Rousseau and Ashcroft as a heuristic tool for electride formation in Na[25]. In each case, the key physical insight is a substan-

tial constraint on the valence electron wavefunctions over a fixed volume per atom, independent of overall atomic density.

These results establish that calculations of the momentum density function for WDM must necessarily include nonperturbative effects of the electron-ion interaction at the level of wavefunctions or Green's function propagators even well before electride formation is reached. We now discuss the consequences of this observation. First, a full understanding of the consequences of VCO on the EOS or thermodynamic susceptibilities, especially the compressibility, will require further work. That being said, the strong non-free-electron-like modification of $n(p)$, and thus also the kinetic energy[48], with compression makes it clear that its consequences cannot, *a priori*, be ignored.

Second, moving to experimental consequences, we return to Fig. 3 where, for the highest-density calculations, we show a fit to the RSGF predictions using the BMA with adjustable $\rho$ and $T$. The large weight in the RSGF tail is reproduced by the BMA model only when increasing the density by 30% and increasing the temperature from 0 to 8 eV. While the exact consequences for interpretation or reinterpretation of experiment will require further work, the message is clear: failure to include the effects of VCO will result in a systematic overestimate of either $T$, $n_e$, or both.

In Fig. 4 we compare RSGF and BMA valence contributions to synthetic NIXS spectra under the following four thermodynamic conditions: (a) ambient, (b) isochoric heating, (c) isothermal compression, and (d) shock-compression/heating. High-temperature RSGF calculations were performed by using a finite-temperature exchange-correlation potential[49] and using the Fermi distribution for the occupation of states both in the self-consistency loop and in the final calculation of the Compton profile.[50] The ionic lattice was kept ordered. All curves have been broadened by a 5-eV FWHM Gaussian. At this resolution, which is attainable using the seeded source at LCLS, the effects of VCO on the Compton profile should be measurable.

One interesting future direction is to investigate the corresponding momentum-space phenomenon associated with the real-space segregation of valence charge density in proposed electride phases. It may be the case that electride formation can be more easily observed, especially in disordered systems, by its influence on $n(p)$ rather than by its slight modification of the static structure factor $S(q)$ in elastic scattering.

In conclusion, we have shown that non-perturbative effects of the electron-ion interaction, such as core-valence orthogonalization, play an increasingly important role in determining the momentum distribution of free electrons in ordered dense matter as density is increased. This will have a profound effect on the interpretation of NIXS-based diagnostic measurements of WDM, and may also be relevant for thermodynamic properties of dense, partially ionized plasmas.

This work was supported by the US Department of Energy, Office of Science, Fusion Energy Sciences and the National Nuclear Security Administration, through grant DE-SC0008580. We thank J. J. Rehr, S. Huotari and S. Hanson for many helpful discussions.

* seidler@uw.edu

[1] G. Huser, M. Koenig, A. Benuzzi-Mounaix, E. Henry, T. Vinci, B. Faral, M. Tomasini, B. Telaro, and D. Batani, Physics of Plasmas **12**, 060701 (2005).
[2] N. Amadou, E. Brambrink, A. Benuzzi-Mounaix, G. Huser, F. Guyot, S. Mazevet, G. Morard, T. de Resseguier, T. Vinci, K. Myanishi, N. Ozaki, R. Kodama, T. Boehly, O. Henry, D. Raffestin, and M. Koenig, High Energy Density Physics **9**, 243 (2013).
[3] B. A. Remington, R. P. Drake, and D. D. Ryutov, Reviews of Modern Physics **78**, 755 (2006).
[4] H. F. Wilson and B. Militzer, Phys. Rev. Lett. **108**, 111101 (2012).
[5] J. D. Lindl, P. Amendt, R. L. Berger, S. G. Glendinning, S. H. Glenzer, S. W. Haan, R. L. Kauffman, O. L. Landen, and L. J. Suter, Physics of Plasmas **11**, 339 (2004).
[6] S. H. Glenzer and R. Redmer, Reviews of Modern Physics **81**, 1625 (2009).
[7] R. Redmer and G. Röpke, Contributions to Plasma Physics **50**, 970 (2010).
[8] T. Sjostrom, F. E. Harris, and S. B. Trickey, Phys. Rev. B **85**, 045125 (2012).
[9] V. V. Karasiev, T. Sjostrom, and S. B. Trickey, Phys. Rev. E **86**, 056704 (2012).
[10] V. V. Karasiev, T. Sjostrom, and S. B. Trickey, Phys. Rev. B **86**, 115101 (2012).
[11] G. Gregori, S. H. Glenzer, W. Rozmus, R. W. Lee, and O. L. Landen, Phys. Rev. E **67**, 026412 (2003).
[12] G. Gregori, S. H. Glenzer, F. J. Rogers, S. M. Pollaine, O. L. Landen, C. Blancard, G. Faussurier, P. Renaudin, S. Kuhlbrodt, and R. Redmer, Physics of Plasmas **11**, 2754 (2004).
[13] D. Bohm and D. Pines, Phys. Rev. **92**, 609 (1953).
[14] A. Selchow, G. Röpke, A. Wierling, H. Reinholz, T. Pschiwul, and G. Zwicknagel, Phys. Rev. E **64**, 056410 (2001).
[15] N. D. Mermin, Phys. Rev. B **1**, 2362 (1970).
[16] H. J. Lee, P. Neumayer, J. Castor, T. Döppner, R. W. Falcone, C. Fortmann, B. A. Hammel, A. L. Kritcher, O. L. Landen, R. W. Lee, D. D. Meyerhofer, D. H. Munro, R. Redmer, S. P. Regan, S. Weber, and S. H. Glenzer, Phys. Rev. Lett. **102**, 115001 (2009).
[17] A. L. Kritcher, T. Döppner, C. Fortmann, T. Ma, O. L. Landen, R. Wallace, and S. H. Glenzer, Phys. Rev. Lett. **107**, 015002 (2011).
[18] C. Fortmann, H. J. Lee, T. Döppner, R. W. Falcone, A. L. Kritcher, O. L. Landen, and S. H. Glenzer, Phys. Rev. Lett. **108**, 175006 (2012).
[19] T. Ma, T. Döppner, R. W. Falcone, L. Fletcher, C. Fortmann, D. O. Gericke, O. L. Landen, H. J. Lee, A. Pak, J. Vorberger, K. Wünsch, and S. H. Glenzer, Phys. Rev.

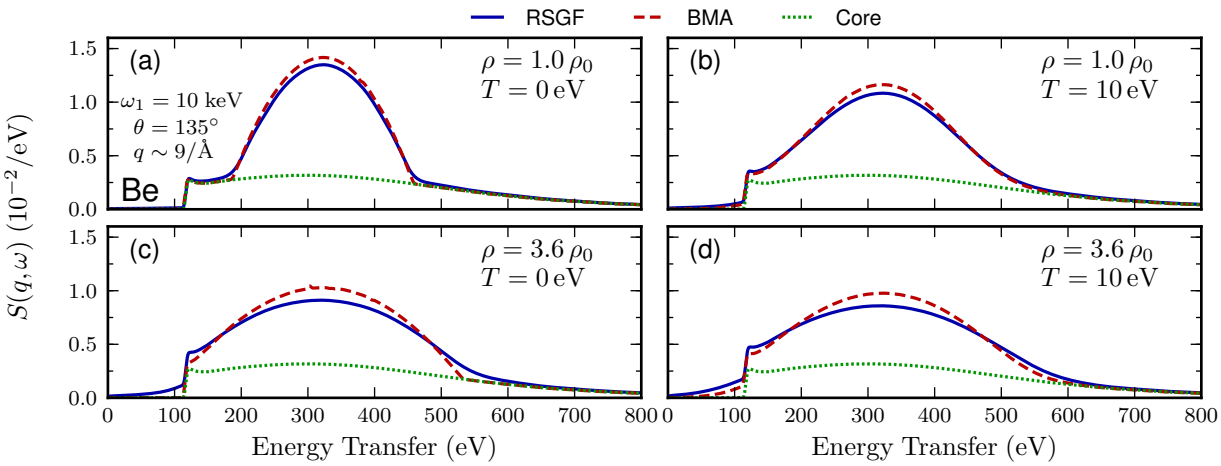



FIG. 4. Simulated NIXS spectra. (a) Ambient density and temperature (b) Isochoric heating (c) Adiabatic compression (d) Shock Compression/Heating. All curves are for a 10-keV incident energy at 135° scattering angle and include 5-eV broadening.


Lett. **110**, 065001 (2013).
[20] F. Bloch, Zeitschrift für Physik **52**, 555 (1929).
[21] N. W. Ashcroft and D. N. Mermin, *Solid state physics*, 1st ed. (Thomson Learning, Toronto, 1976).
[22] N. W. Ashcroft and J. Lekner, Phys. Rev. **145**, 83 (1966).
[23] J. B. Neaton and N. W. Ashcroft, Nature **400**, 141 (1999).
[24] J. B. Neaton and N. W. Ashcroft, Phys. Rev. Lett. **86**, 2830 (2001).
[25] B. Rousseau and N. W. Ashcroft, Phys. Rev. Lett. **101**, 046407 (2008).
[26] L. D. Landau and E. Lifshitz, *Statistical Physics I*, Course of theoretical physics (Elsevier, Amsterdam, 1980) p. 168.
[27] K.-U. Plagemann, P. Sperling, R. Thiele, M. P. Desjarlais, C. Fortmann, T. Döppner, H. J. Lee, S. H. Glenzer, and R. Redmer, New Journal of Physics **14**, 055020 (2012).
[28] J. Vorberger and D. Gericke, High Energy Density Physics **9**, 178 (2013).
[29] M. Itou, Y. Sakurai, T. Ohata, A. Bansil, S. Kaprzyk, Y. Tanaka, H. Kawata, and N. Shiotani, Journal of Physics and Chemistry of Solids **59**, 99 (1998).
[30] S. Huotari, K. Hämäläinen, S. Manninen, S. Kaprzyk, A. Bansil, W. Caliebe, T. Buslaps, V. Honkimäki, and P. Suortti, Physical Review B **62**, 7956 (2000).
[31] S. Huotari, C. Sternemann, M. Volmer, J. A. Soininen, G. Monaco, and W. Schülke, Phys. Rev. B **76**, 235106 (2007).
[32] S. Huotari, J. A. Soininen, T. Pylkkänen, K. Hämäläinen, A. Issolah, A. Titov, J. McMinis, J. Kim, K. Esler, D. M. Ceperley, M. Holzmann, and V. Olevano, Phys. Rev. Lett. **105**, 086403 (2010).
[33] C. Herring, Phys. Rev. **57**, 1169 (1940).
[34] P. E. Blöchl, Phys. Rev. B **50**, 17953 (1994).
[35] K. Pandey and L. Lam, Physics Letters A **43**, 319 (1973).
[36] M. Cooper, P. Pattison, B. Williams, and K. C. Pandey, Philosophical Magazine **29**, 1237 (1974).
[37] P. Rennert, Phys. Stat. Sol. B **105**, 567 (1981).
[38] L. Bellaiche and K. Kunc, Phys. Rev. B **55** (1997).
[39] W. Schülke, *Electron Dynamics by Inelastic X-Ray Scattering*, Oxford Series on Synchrotron Radiation (Oxford University Press, New York, 2007).
[40] P. Eisenberger and P. M. Platzman, Physical Review A **2**, 415 (1970).
[41] B. A. Mattern and G. T. Seidler, Physics of Plasmas **20**, 022706 (2013).
[42] See Supplemental Information.
[43] J. J. Kas, J. J. Rehr, and L. Reining, *To be submitted* Phys. Rev. Lett. (2013).
[44] L. X. Benedict, T. Ogitsu, A. Trave, C. J. Wu, P. A. Sterne, and E. Schwegler, Phys. Rev. B **79**, 064106 (2009).
[45] B. A. Mattern, G. T. Seidler, J. J. Kas, J. I. Pacold, and J. J. Rehr, Phys. Rev. B **85**, 115135 (2012).
[46] J. J. Rehr, J. J. Kas, M. P. Prange, A. P. Sorini, Y. Takimoto, and F. Vila, Comptes Rendus Physique **10**, 548 (2009).
[47] J. J. Rehr and R. C. Albers, Rev. Mod. Phys. **72**, 621 (2000).
[48] I. R. Epstein, Phys. Rev. A **8**, 160 (1973).
[49] F. m. c. Perrot and M. W. C. Dharma-wardana, Phys. Rev. A **30**, 2619 (1984).
[50] B. A. Mattern, *Compton Scattering and Warm Dense Matter Thermometry*, Ph.D. thesis, University of Washington, Seattle (2013).